Why Direct Tension Test Specimens Break Flexing to the Side

By Zdeněk P. Bažant,[1] Fellow, ASCE, and Luigi Cedolin,[2] Member, ASCE

Abstract: Contrary to the traditional view, unnotched direct tension test specimens of quasi-brittle materials that exhibit post-peak strain softening do not deform symmetrically. After passing the peak load, the equilibrium path bifurcates and the secondary postbifurcation branch represents flexing to the side. The bifurcation is shown to be analogous to Shanley's bifurcation in elastoplastic columns. According to the thermodynamic criterion of stable path, the flexing to one side must occur even if the geometry is perfect and if the straightening effect of the moment of the axial force about the centroid of the deflected cross section is taken into account. The lateral flexing favors failure of the specimen at midlength. The phenomenon (which is similar to the recently discovered behavior of notched tensile fracture specimens) is first illustrated using a simple model in which the specimen consists of two rigid bars of unequal lengths, joined by a strain-softening link. It is shown that flexing to the side is retarded if the attachments to the loading machine exert a sufficient restraint against rotation. The analysis is then extended to a specimen consisting of two unloading elastic beams joined by a short strain-softening segment, and similar conclusions are reached. The maximum load in the unnotched direct-tension test gives the material strength limit, but the postpeak load-deflection response cannot yield the strain-softening material properties and energy-absorption capability except when sophisticated stability analysis is made and the size of the strain-softening zone is known a priori.

Introduction

The direct tensile test is widely used for determining the uniaxial yield limit or direct tensile strength of a material. However, for brittle or quasi-brittle materials, such as concrete, rock, or ceramics, which exhibit strain softening, the interpretation of this test is not easy.

As van Mier (1986, 1989), Rots and de Borst (1987, 1989), and Hordijk et al. (1987) have shown, both by experiment and by numerical finite-element analysis with the crack-band model, symmetrically notched prismatic specimens subjected to centric tension do not deform symmetrically but flex to one side as cracks propagate from the notches. A similar loss of symmetry and lateral flexing was analytically demonstrated on the basis of linear elastic fracture mechanics in Bažant (1988, 1989) and Bažant and Tabbara (1989). The conclusion was that only one of the two symmetric cracks can propagate. Subsequently Bažant (unpublished lectures, 1989) and Bažant and Cedolin [(1991) section 13.8] analyzed bifurcation and the stable response path of the centrically tensioned specimen shown in Fig. 1, which consists of two rigid bars of equal length that are restrained at the ends by springs and are connected in the middle by two softening elements. They found that this idealized specimen, too, flexes to one side if certain not abnormal conditions are met. A similar phenomenon was demonstrated by Pijaudier-Cabot and Akrib (1989), who used layered beam finite elements

[1]Walter P. Murphy Prof. of Civ. Engrg., Northwestern Univ., Evanston, Ill 60208.
[2]Prof. of Struct. Engrg., Politecnico di Milano, Piazza Leonardo da Vinci, 32, Milano 20133, Italy.

Note. Discussion open until September 1, 1993. To extend the closing date one month, a written request must be filed with the ASCE Manager of Journals. The manuscript for this paper was submitted for review and possible publication on December 23, 1991. This paper is part of the ***Journal of Structural Engineering***, Vol. 119, No. 4, April, 1993. ©ASCE, ISSN 0733-9445/93/0004-1101/$1.00 + $.15 per page. Paper No. 3179.

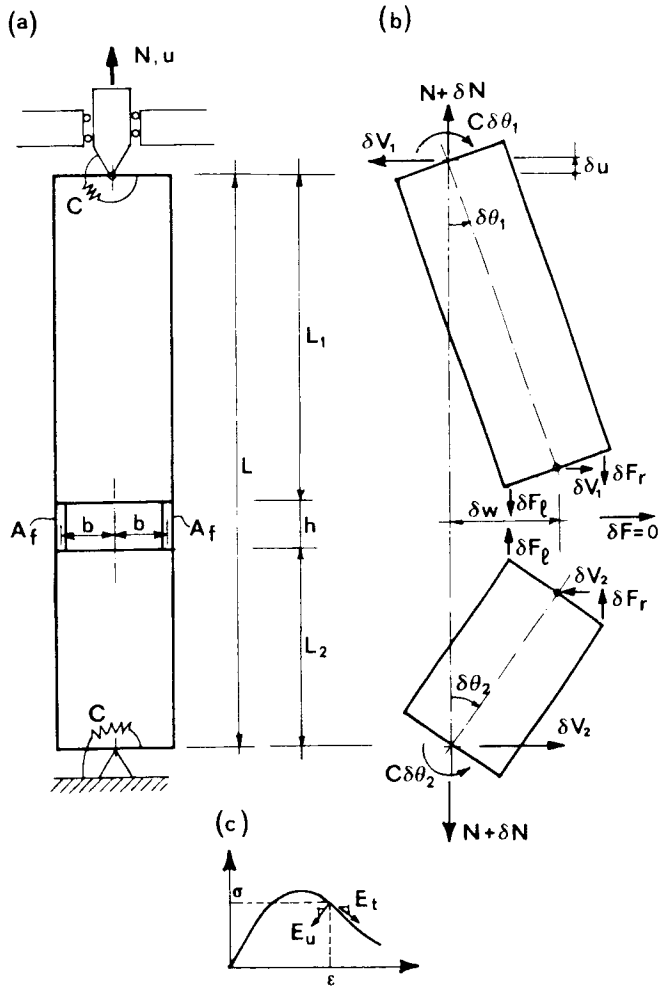

FIG. 1. (*a*) Rigid-Bar Model of Direct Tension Specimen; (*b*) Free-Body Diagram; (*c*) Loading and Unloading Tangential Moduli

to analyze a tensile specimen with strain-softening due to distributed cracking.

The previous finite-element analysis of the lateral flexing of tensile specimens neglected the second-order geometric effects of lateral deflections. While in compression these effects promote lateral deflection of the specimen, in tension they retard it because the moment of the axial tensile force about the centroid of the deflected cross section at midlength tends to straighten the specimen. The more slender the specimen, the more pronounced this effect must be. Thus there arises the question of whether the nonlinear geometric effects might be able to prevent lateral flexing. We will see that in general they cannot.

The objective of this paper is to generalize the solution of Bažant (unpublished lectures, 1989) and Bažant and Cedolin (1991), present a simple, convincing demonstration of the loss of symmetry of response, and discuss in simple, easily comprehensible terms the practical implications for the direct tension test.

Flexing of Specimen Consisting of Two Rigid Bars

Incremental Equilibrium Equations

For the sake of simple illustration we consider the tensile specimen in Fig. 1(*a*). Let N be the axial (tensile) load and u the corresponding axial displacement. The bar length is L, and we let the two rigid bars have, in general, unequal lengths L_1 and L_2. The bars are linked by two deformable short flanges of length h ($h \ll L$; $L = L_1 + L_2$) and cross-section areas A_f, each of negligible width and located at distances b from the cross-section center. These flanges, in which the strain is assumed to be uniform, can exhibit strain-softening, characterized by tangent softening modulus E_t [$E_t < 0$; Fig. 1(*c*)]. The specimen is supported at the ends by hinges with springs of rotational stiffnesses C. Let w be the deflection of the link, and θ_1 and θ_2 the inclination angles of bars L_1 and L_2, respectively. The link is assumed to transmit a shear force without deforming in shear.

Let us assume that initially $\theta_1 = \theta_2 = 0$ (which means the structure is perfect), and that the equilibrium is disturbed by applying a small lateral load δF at the link, while the axial tensile force varies by δN [Fig. 1(*b*)]. The flange on the right side follows the loading modulus E_t ($E_t < 0$), while the flange on the left side obeys modulus ξE_t, with $\xi = 1$ if its strain is increasing or remaining constant and $\xi = E_u/E_t$ if the strain is decreasing; E_u is the unloading modulus [Fig. 1(*c*)] ($0 < E_u \leq E$ = initial elastic modulus). The equilibrium conditions of each bar for vertical forces and for moments about the center of the link require that $\delta F_l + \delta F_r = \delta N$ and $b(\delta F_l - \delta F_r) = N\delta w + C\delta\theta_1 - \delta V_1 L_1$, where $\delta V_1 = \delta F(L_2/L) - (C/L)(\delta\theta_2 - \delta\theta_1)$; and δF_l, δF_r = variation of forces in the left and right flanges, given by $\delta F_l = E_u A_f \delta\varepsilon_l$; and $\delta F_r = E_t A_f \delta\varepsilon_r$. The strains in the left and right flanges of the link are $\delta\varepsilon_l = (\delta u/h) - b(\delta\theta_1 + \delta\theta_2)/h$; and $\delta\varepsilon_r = (\delta u/h) + b(\delta\theta_1 + \delta\theta_2)/h$. From the compatibility conditions, $\delta w = \delta\theta_1 L_1 = \delta\theta_2 L_2$. Eliminating $\delta\varepsilon_l$, $\delta\varepsilon_r$, $\delta\theta_1$, $\delta\theta_2$, δF_l, δF_r, and δV_1 from these equations, we obtain

$$\mathbf{K}\delta\mathbf{q} = \delta\mathbf{F} \qquad (1a)$$

or

$$\begin{bmatrix} K_{11} & K_{12} \\ K_{21} & K_{22} \end{bmatrix} \begin{bmatrix} \delta u \\ \delta w \end{bmatrix} = \begin{bmatrix} \delta N \\ \delta F \end{bmatrix} \qquad (1b)$$

where $\mathbf{K}$ = tangential stiffness matrix, the elements of which are

$$K_{11} = \frac{A_f E_t}{h}(1 + \xi) \qquad (2a)$$

$$K_{12} = K_{21} = \frac{A_f E_t b L}{h L_1 L_2}(1 - \xi) \qquad (2b)$$

$$K_{22} = \frac{A_f E_t b^2 L^2}{h L_1^2 L_2^2}(1 + \xi) + \frac{L}{L_1 L_2}\left(N + \frac{C(L_1^2 + L_2^2)}{L L_1 L_2}\right) \qquad (2c)$$

with $\delta\mathbf{q} = (\delta u, \delta w)^T$ and $\delta\mathbf{F} = (\delta N, \delta F)^T$.

A comment on our choice of variations is in order. If we investigated only the stability of equilibrium states, then we could consider only one variation, δw, since the assumption of a displacement-controlled test implies that $\delta u = 0$ (displacement control is necessary for being able to observe postpeak states). In inelastic structures, however, bifurcations typically do not occur at the moment of stability loss, but earlier. Here we are interested mainly in bifurcation of equilibrium path, which can happen during a controlled variation (increment), δu, of the axial displacement [for detailed explanation and examples of similar problems see Bažant and Cedolin (1991), chapter 10]. So we must consider two variations, δw and δu.

First Bifurcation: No Unloading

If the tangential modulus E_t varies continuously, the first bifurcation may be expected to occur while there is no unloading in the structure, i.e. $\xi = 1$ [see Bažant and Cedolin (1991), chapter 10]. For the primary path ($w = 0$) we have $\mathbf{K}\delta\mathbf{q}^{(1)} = \delta\mathbf{F}$ and for the secondary path ($w \neq 0$) we have $\mathbf{K}\delta\mathbf{q}^{(2)} = \delta\mathbf{F}$. If there is bifurcation, these two equations must be satisfied simultaneously for the same $\delta\mathbf{F}$, and since there is no unloading, matrices $\mathbf{K}$ are the same in both equations. Subtracting them, we get $\mathbf{K}[\delta\mathbf{q}^{(2)} - \delta\mathbf{q}^{(1)}] = \mathbf{0}$. This is a system of linear equations for $[\delta\mathbf{q}^{(2)} - \delta\mathbf{q}^{(1)}]$, and if there is bifurcation, $\delta\mathbf{q}^{(2)} - \delta\mathbf{q}^{(1)} \neq 0$, which occurs if and only if $\det\mathbf{K} = 0$. This is the condition of first bifurcation [e.g. Bažant and Cedolin (1991), section 10.4], which was in plasticity formulated by Hill (1958). Note, however, that $\det\mathbf{K} = 0$ also occurs at the limit point (maximum point) of the equilibrium path, in which case $\det\mathbf{K} = 0$ does not imply bifurcation.

Let us assume that the equilibrium path [Fig. 2(*a*)] is followed by incrementing displacement u (displacement control) while the lateral disturbing force $\delta F = 0$. Before the axial load N reaches its maximum, $E_t > 0$, $\xi = 1$, $K_{12} = K_{21} = 0$, $\det\mathbf{K} > 0$, and, because $\delta F = 0$, we have $\delta w = 0$; that is, the system follows a symmetric (primary) equilibrium path. At $N = N_{\max}$, $E_t = 0$, and, consequently, $K_{11} = K_{12} = K_{21} = 0$ and $\det\mathbf{K} = 0$. However δu is controlled and, since $K_{22} > 0$, $\delta w = 0$; that is, no deflection can occur. Therefore, the first point at which $\det\mathbf{K}$ vanishes is not a bifurcation point but the limit point [$N_{\max}$ in Fig. 2(*a*)]. When the axial displacement is increased further, the tangent modulus E_t becomes negative; the load decreases, but no deflection is possible until again $\det\mathbf{K} = 0$. For no unloading ($\xi = 1$), this condition is equivalent to $K_{11}K_{22} = 0$ or $K_{22} = 0$, which gives

$$-E_t = \frac{hL_1L_2}{2b^2LA_f}\left(N + \frac{C(L_1^2 + L_2^2)}{LL_1L_2}\right) = |E_t|_{cr} \qquad (3)$$

In this case

$$\delta N = K^{(1)}\delta u \qquad (4a)$$

$$K^{(1)} = \frac{2A_fE_t}{h} \qquad (4b)$$

and δw is arbitrary, subject only to the loading condition $\delta\varepsilon_f \geq 0$, which, by substitution of the expression $\delta\theta_1 + \delta\theta_2 = \delta w(L/L_1L_2)$, becomes

$$\mu = \frac{\delta w}{\delta u} \leq \frac{L_1L_2}{bL} \qquad (5)$$

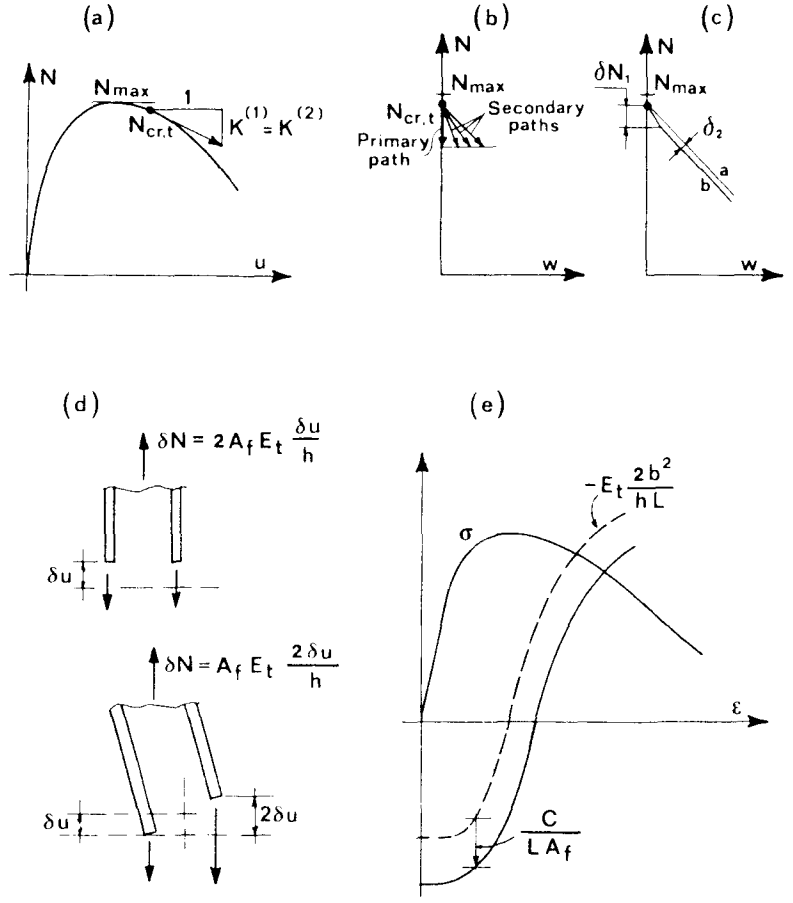

FIG. 2. (*a–c*) Bifurcation of Equilibrium Path; (*d*) Equilibrium Condition in Flanges for Primary and Secondary Path; (*e*) Graphical Solution of (12)

We then have for a given finite δu infinitely many possible δw [see Fig. 2(*b*)]. In other words we have a bifurcation of the equilibrium path; there exists a secondary (symmetry breaking) branch, for which the specimen flexes to the side, with a maximum slope in the (N, w) plane, given by $\delta N/\delta w = 2A_fE_tbL/hL_1L_2$. We see that, indeed, the secondary path at first bifurcation occurs at no unloading. This is a rather general property of first bifurcation in inelastic solids (known in plastic buckling as Hill's hypothesis of a linear comparison solid).

The condition expressed by (3) can be cast in the form

$$|E_t|_{cr} = \frac{h}{4b^2A_f}\left[N\frac{L}{2} + C - 2\Delta^2\left(\frac{N}{L} - 2\frac{C}{L^2}\right)\right] \qquad (6)$$

where $\Delta = (L_1 - L_2)/2$ = distance of the location of the link from the specimen midlength. From this expression one can see that $|E_t|_{cr}$: (1) In-

creases with the value of C, i.e. with the stiffness of the rotational restraints at the bar ends; and (2) increases with distance Δ, provided that

$$C > \frac{NL}{2} \quad \ldots\ldots (7)$$

i.e., that the stiffness of the rotational restraint at the bar ends exceeds a certain limit. If this condition is met, the minimum value of $|E_t|_{cr}$ occurs for $L_1 = L_2$, and is given by

$$\min|E_t|_{cr} = \frac{\left(\frac{NL}{2} + C\right) h}{4b^2 A_f} \quad \ldots\ldots (8)$$

Behavior after First Bifurcation: Loading-Unloading

After the first bifurcation, aside from the loading-only (symmetry-preserving) path, a loading-unloading (symmetry-breaking) path become possible. Assuming again that $\delta F = 0$, (1*b*) gives

$$\mu = \frac{\delta w}{\delta u} = -\frac{K_{21}}{K_{22}} = \frac{E_u - E_t}{\frac{h}{bA_f}\left(N + \frac{C(L_1^2 + L_2^2)}{L_1 L_2 L}\right) + \frac{bL}{L_1 L_2}(E_u + E_t)} \quad \ldots\ldots (9)$$

Substituting this into (1*a*), one gets

$$\delta N = K^{(2)} \delta u \quad \ldots\ldots (10a)$$

$$K^{(2)} = \frac{A_f}{h}\left[(E_u + E_t) - \mu(E_u - E_t)\frac{bL}{L_1 L_2}\right] \quad \ldots\ldots (10b)$$

It may be easily checked that, for $(-E_t) \to |E_t|_{cr}$, $\delta w/\delta u \to L_1 L_2/bL$, i.e., after an infinitely small load decrement δN_1 of arbitrary direction [Fig. 2(*c*)], the loading-unloading path starts with a slope equal to the limit slope of the loading-only path. Remembering (5), this means that the limit value of E_t for which the loading-unloading path becomes possible can be calculated by imposing $\delta\varepsilon_t = 0$. We find also that in this case $K^{(2)} \to 2A_f E_t/h = K^{(1)}$. [For an ideal I-section, which is considered here, the condition $\delta\varepsilon_t = 0$ for the deflected configuration implies a priori the aforementioned equality of the tangent stiffnesses; see Fig. 2(*d*).]

Path Stability and Actual Behavior of Tensile Test Specimens

According to the thermodynamic condition of stable postbifurcation branch given in Bažant and Cedolin [(1991) sections 10.2–10.3], the equilibrium branch that must occur is that for which the tangent slope given by $K^{(1)}$ or $K^{(2)}$ is steeper. Thus, the symmetry-breaking secondary branch first can occur when $K^{(1)} = K^{(2)}$ and must occur when

$$K^{(2)} < K^{(1)} \quad \ldots\ldots (11)$$

From (9) and (10) one finds that the condition given by (11) is always satisfied for $E_t < -|E_t|_{cr}$. Consequently, assuming the softening stress-strain diagram to have a gradually steepening downward slope, the specimen will flex to

the side as soon as the condition $E_t = -|E_t|_{cr}$ is exceeded, i.e. E_t becomes less than $-|E_t|_{cr}$, which happens immediately after the first bifurcation point.

The rigid-bar specimen that we analyzed may be imagined to approximate the behavior in actual direct tension tests. Contrary to fracture specimens with notches, the location of the failure zone within the specimen length is indeterminate if deflection to the side is ignored (it then depends on the randomness of material properties, or, if failure occurs near the grips, it may be attributed to stress concentrations due to poor grips or to poor gluing of the specimen ends to the platens).

As the foregoing analysis shows, if there is a rotational restraint of nonzero stiffness at the specimen ends, the minimum magnitude $|E_t|_{cr}$ of the tangent modulus for which flexing to the side occurs is attained when the specimen breaks in the middle. Moreover, it increases with C. It follows that, in order to increase stability of the primary path, one should increase the stiffness of the rotational restraints at the bar ends.

If no restraints at the specimen ends are present ($C = 0$), the value of $|E_t|_{cr}$ given by (3) tends to zero when the failure zone occurs near the ends, and attains a finite value $|E_t|_{cr} = (hNL)(8b^2 A_f)$ when the failure zone is located in the middle. This means that, in absence of rotational restraints, the specimen fails right at the peak load and failure occurs at the ends.

Analogy with Shanley's Tangent Modulus Load of Elastoplastic Column

For the case $L_1 = L_2 = L$, the condition expressed by (3) can be cast in the form

$$-E_t \frac{2b^2}{hL} - \frac{C}{LA_f} = \sigma \quad \ldots\ldots (12)$$

where we have put $\sigma = N/2A_f$. This is an implicit equation exactly analogous to that defining Shanley's tangent modulus load of a compressed elastoplastic column (Shanley 1947) [for a review, see for example Bažant and Cedolin (1991), sections 8.1 and 10.2–10.4, Hill (1958, 1961), and Hutchinson (1974)]. Fig. 2(*e*), drawn for a generic stress-strain law, shows the graphical solution of (12). We again see that the effect of the spring stiffness C is that an increase of C prolongs the stable path beyond the peak.

We must note, however, that while in compression, the Shanley's load corresponds to a bifurcation of the equilibrium path (which can be reached under both load control and displacement control), in tension the bifurcation load defined by (12) can be reached only under displacement control, because under load control the specimen would fail at the peak load [N_{max} in Fig. 2(*a*)]. We must also point out that while in compression, the loss of stability of the undeflected state (neutral equilibrium at bifurcation) occurs after the first bifurcation (and corresponds to different critical loads depending on the type of control; see Bažant (1988, 1989a,b) or Bažant and Cedolin (1991), section 10.3], in tension it cannot occur (except, as already mentioned, as a limit point). This can be easily understood by realizing that, with a negative slope of the loading branch, both flanges give a negative contribution to the axial load, i.e. neutral equilibrium is not possible. This can also be shown by introducing the condition of unloading of the left flange, expressed by the opposite of (5), into (10); the resulting value of $K^{(2)}$ is always <0.

Overall we may conclude that the strain-softening feature of the constitutive law engenders bifurcation of the equilibrium path in direct tensile

test, a fact that has not been suspected. The popular wisdom has been that buckling to the side can be caused by compression only, but in the case of softening behavior this is now seen to be false.

Elastic Specimen with Strain-Softening Slice

A more realistic analysis requires consideration of a deformable specimen, as shown in Fig. 3(*a*). This specimen, of length L, has a rectangular cross section of depth r and width s, and is restrained at both ends by springs of stiffness C. We assume that strain-softening, if it occurs, must be localized in a beam slice of a short length h ($h \ll L$), located at distances L_1 and L_2 from the specimen top and bottom [Fig. 3(*a*)]; $L_1 + L_2 \simeq L$ = specimen length. Let E_t ($E_t < 0$) be the tangent modulus for loading and E_u ($E_u > 0$) be the modulus for unloading [Fig. 3(*d*)] at the moment when the symmetry-breaking bifurcation with strain softening in the slice begins. Outside the slice, there is no loading anywhere. The variations of the rotations of the ends of the slice at the moment of bifurcation are denoted as $\delta\theta_1$ and $\delta\theta_2$. The variation of curvature in the slice is

$$\delta\kappa = \frac{\delta\theta_1 + \delta\theta_2}{h} \qquad \text{(13)}$$

The variations of strains at the left and right faces of the slice are $c\delta\kappa$ and $(s - c)\delta\kappa$, where c is the distance from the left face to the neutral axis, which separates loading from unloading [Fig. 3(*c*)]. Since in the rigid-bar model previously presented we have seen that the limit condition for the existence of the symmetry-breaking path is $\delta\varepsilon_t = 0$, we will use in the deformable-bar model the condition $c = 0$ in order to determine the critical value of E_t.

Let x be the axial coordinate measured from the top, $I = rs^3/12$, and w be the deflection curve. The differential equation of beam column is $E_u I(d^4w/dx^4) - N(d^2w/dx^2) = 0$ (N being positive for tension), and its general solution under the boundary conditions $w = 0$ and $E_u I d^2w/dx^2 = C dw/dx$ at the top ($x = 0$) is $w = A_1(\sinh kx + \psi k \cosh kx - \psi k) + B_1(x + \psi \cosh kx - \psi)$, where $k^2 = N/E_u I$ and $\psi = C/E_u I k^2$. Compatibility with the rotation variation at the slice requires that $dw/dx = \delta\theta_1$ at $x = L_1$, i.e.

$$A_1 k(\cosh kL_1 + \psi k \sinh kL_1) + B_1(1 + \psi k \sinh kL_1) = \delta\theta_1 \qquad \text{(14)}$$

Similarly, for bar segment L_2

$$A_2 k(\cosh kL_2 + \psi k \sinh kL_2) + B_2(1 + \psi k \sinh kL_2) = \delta\theta_2 \qquad \text{(15)}$$

Compatibility of deflection variations at the top and bottom of the slice requires that, for small h, $\delta w_1 = \delta w_2$, i.e.

$$A_1(\sinh kL_1 + \psi k \cosh kL_1 - \psi k) + B_1(L_1 + \psi \cosh kL_1 - \psi)$$
$$= A_2(\sinh kL_2 + \psi k \cosh kL_2 - \psi k) + B_2(L_2 + \psi \cosh kL_2 - \psi) \qquad \text{(16)}$$

The shear-force variation at the slice is $\delta V = -\delta M' + N\delta w'$. For the variations of the bending moment M and the shear force V at the top and bottom of the slice we have the equilibrium conditions

$$\delta M = E_u I k^2[A_1(\sinh kL_1 + \psi k \cosh kL_1) + B_1\psi \cosh kL_1] \qquad \text{(17a)}$$

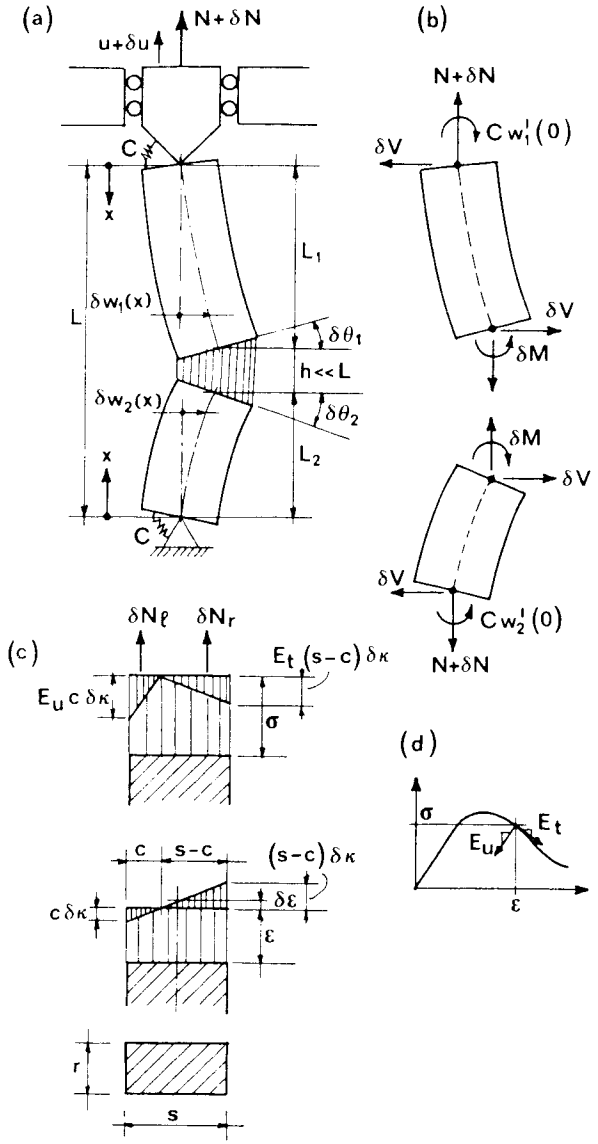

FIG. 3. (*a*) Deformable-Bar Model; (*b*) Free-Body Diagram; (*c*) Variations of Stresses and Strains throughout Strain-Softening Slice; (*d*) Loading and Unloading Tangential Moduli

$$\delta M = E_u I k^2[A_2(\sinh kL_2 + \psi k \cosh kL_2) + B_2\psi \cosh kL_2] \qquad \text{(17b)}$$

$$A_1[-E_u I k^3(\cosh kL_1 + \psi k \sinh kL_1) + Nk(\cosh kL_1 + \psi k \sinh kL_1)]$$
$$+ B_1[-E_u I k^3 \psi k \sinh kL_1 + Nk(1 + \psi k \sinh kL_1)]$$

$$+ A_2[-E_u Ik^3(\cosh kL_2 + \psi k \sinh kL_2) + Nk(\cosh kL_2 + \psi k \sinh kL_2)]$$

$$+ B_2[-E_u Ik^3 \psi k \sinh kL_2 + Nk(1 + \psi k \sinh kL_2)] = 0 \quad \ldots\ldots (18)$$

The variation of the axial force resultant of the stresses in the slice and the variation of the bending moment about the cross section center are [Fig. 3(*c*)]

$$\delta N = \delta N_t + \delta N_r \quad \ldots\ldots (19a)$$

$$\delta M = \left(\frac{s}{2} - \frac{c}{3}\right) \delta N_t - \left(\frac{s}{2} - \frac{s-c}{3}\right) \delta N_r \quad \ldots\ldots (19b)$$

where

$$\delta N_t = -E_u c \delta\kappa \frac{c}{2} r \quad \ldots\ldots (20a)$$

$$\delta N_r = E_t(s-c)\delta\kappa \frac{s-c}{2} r \quad \ldots\ldots (20b)$$

Finally, the variation of the axial strain of the slice, $\delta\varepsilon$, is expressed by

$$\delta\varepsilon = \frac{\delta u}{h} \quad \ldots\ldots (21a)$$

$$\delta\varepsilon = \left(\frac{s}{2} - c\right) \delta\kappa \quad \ldots\ldots (21b)$$

Eqs. (13)–(21) represent a system of 13 equations for the unknowns δN, δN_t, δN_r, δM, c, A_1, B_1, A_2, B_2, $\delta\theta_1$, $\delta\theta_2$, $\delta\kappa$, and $\delta\varepsilon$, with δu prescribed. This equation system may be solved as follows. First we obtain the ratios $\alpha = B_1/A_1$, $\beta = A_2/A_1$, and $\gamma = B_2/A_1$ from (16), (17*b*), and (18). Substituting now (14) and (15) into (13), we get $A_1 = (h/kG_1)\delta\kappa$, where $G_1 = \cosh kL_1 + \psi k \sinh kL_1 + \alpha(\psi \sinh kL_1 + 1/k) + \beta(\cosh kL_2 + \psi k \sinh kL_2) + \gamma(\psi \sinh kL_2 + 1/k)$. We can at this point express the constants $A_1, \ldots, B_2$ as functions of $\delta\kappa$. Then, substituting (20) into (19*b*) expressing c from (21*b*), and taking into account (17*a*), we get the following nonlinear equation:

$$F\left(\frac{\delta\varepsilon}{\delta\kappa}\right) + \frac{h}{kG_1} G_2 = 0 \quad \ldots\ldots (22)$$

where F = function of the ratio $\delta\varepsilon/\delta\kappa = y$ defined as $F(y) = (r/6)[E_u(s/2 - y)^2(s + y) + E_t(s/2 + y)^2(s - y)]$ and $G_2 = E_u Ik^2(\sinh kL_1 + \psi k \cosh kL_1 + \alpha\psi \cosh kL_1)$.

The expression for the tangent stiffness $K^{(2)} = \delta N/\delta u$ may be found by substituting (20) and (21) into (19*a*). We obtain

$$K^{(2)} = \frac{r}{2h}\left[-E_u\left(\frac{s}{2} - \frac{\delta\varepsilon}{\delta\kappa}\right)^2 + E_t\left(\frac{s}{2} - \frac{\delta\varepsilon}{\delta\kappa}\right)^2\right]\left(\frac{\delta\varepsilon}{\delta\kappa}\right)^{-1} \quad \ldots\ldots (23)$$

We can now solve (22) under the condition $0 \le c \le s$ [which assures that the expressions of δN_t and δN_r in (20) are correct] and substitute the solution (if it exists) for $\delta\varepsilon/\delta\kappa$ into (23). This equation gives then the value of $K^{(2)}$,

which may be compared to the tangent stiffness for the primary equilibrium path

$$K^{(1)} = \frac{E_t A}{h} \quad \ldots\ldots (24)$$

in order to tell, according to (11), which equilibrium path will be followed. In the foregoing formulation we neglect both axial deformation of the bars and second-order axial displacements due to deflection.

The limit condition $c = 0$ is equivalent to $(h/2) - (\delta\varepsilon/\delta\kappa) = 0$, which ensues from (21*b*). When this is substituted into (23), one gets for $K^{(2)}$ a value that coincides with $K^{(1)}$, similarly to what we found for the rigid-bar specimen. The corresponding value of E_t is given by

$$-E_t = |E_t|_{cr} = \frac{12G_2 h}{kG_1 rs^3} \quad \ldots\ldots (25)$$

Again one finds that, for $E_t < -|E_t|_{cr}$, (11) is always satisfied.

Numerical calculations show that the effects of the stiffness of the end restraints and of the position of the strain-softening zone along the bar are analogous to those found for the rigid-bar specimen. This is illustrated by Fig. 4, which shows the value of $|E_t|_{cr}$ as a function of the stiffness C for

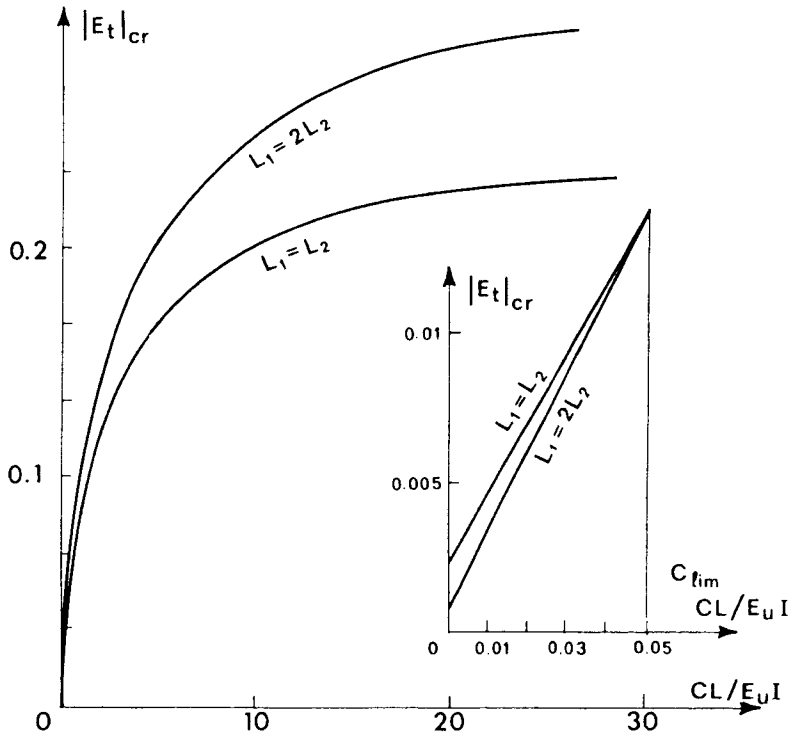

FIG. 4. Minimum Magnitude of Loading Tangential Modulus at Bifurcation for Different Values of L_1/L_2

different values of the ratio L_1/L_2, for the case that $L = 100$ cm; $h = s = 5$ cm; $r = 10$ cm; $I = 500$ cm^3; $N = 15{,}000$ N; and $E_u = 3 \times 10^6$ N/cm^2. One can see that the effect of increasing the stiffness of the end restraints is to enhance the stability of the primary path. One can also see that, below a certain finite value C_{lim}, unequal lengths of the two elastic parts of the specimen are favored because they cause an earlier flexing to the side. The contrary happens for $C > C_{lim}$. Since C_{lim} is usually a very small value, the specimens with rotational end restraints should usually break in the middle, which is a desired behavior in material testing.

Similarly to the previous case of a specimen consisting of two rigid bars, one can calculate the stiffness matrix $\mathbf{K}$ and show that again the first bifurcation follows from the condition $\det\mathbf{K} = 0$.

Imperfect Specimens

The present analysis dealt only with perfect specimens. When the specimen has imperfections, such as the initial deflection or load eccentricity, the equilibrium path shows deflection from the beginning and asymptotically approaches the secondary path of the perfect structure when the deflections become large.

Conclusions

The equilibrium path in a direct tension test of a strain-softening material exhibits a bifurcation in which the secondary, symmetry-breaking branch corresponds to flexing of the specimen to the side. According to the thermodynamic condition for a stable postbifurcation path, the structure must follow the secondary branch.

The occurrence of lateral flexing can be retarded by providing rotational restraints at the specimen ends. The stiffer they are, the steeper the postpeak slope of the strain-softening diagram required for the occurrence of bifurcation.

The analysis shows that lateral flexing favors a break at midlength of the specimen over a break away from the middle.

The bifurcation behavior is analogous to Shanley's bifurcation in elastoplastic columns. But there are differences in stability limits.

Nonlinear geometric effects, particularly the straightening effect of the moment of the axial force about the centroid of the deflected cross section, cannot always prevent the lateral flexing. Imperfections cause lateral flexing already, before the first bifurcation is reached.

Acknowledgment

The general stability analysis was supported under AFOSR grant 91-0140 to Northwestern University, while subsequent applications to concrete testing were supported by the NSF Science and Technology Center for Advanced Cement-Based Materials at Northwestern University, and by Ministero Pubblica Istruzione (grant to Politecnico di Milano).

Appendix. References

Bažant, Z. P. (1988). "Stable states and paths of structures with plasticity or damage." *J. Engrg. Mech.*, ASCE, 114(12), 2013–2034.

Bažant, Z. P. (1989). "Stable states and stable paths of propagation of damage zones and interactive fractures." *Cracking and damage—strain localization and size effect*, J. Mazars and Z. P. Bažant, eds., Elsevier, New York, 183–206.

Bažant, Z. P., and Cedolin, L. (1991). *Stability of structures—elastic, inelastic, fracture, and damage theories*. Oxford University Press, New York, N.Y.

Bažant, Z. P., and Tabbara, M. R. (1989). "Stable propagation of interacting crack systems and modeling of damage." *Trans., 10th Int. Conf. on Struct. Mech. in Reactor Tech. (SMiRT 10)*, A. H. Hadjian, ed., AASMiRT, Los Angeles, Calif., Vol. H, 85–93.

Hill, R. (1958). "A general theory of uniqueness and stability in elastic-plastic solids." *J. Mech. Phys. Solids*, 6, 236–249.

Hill, R. (1961). "Bifurcation and uniqueness in nonlinear mechanics of continua." *Problems of continuum mechanics*, Society of Industrial and Applied Mathematics, Philadelphia, Pa., 155–164.

Hordijk, D. A., Reinhardt, H. W., Cornelissen, H.A.W. (1987). "Fracture mechanics parameters of concrete from uniaxial tensile tests as influenced by specimen length." *Preprints, Conf. on Fracture of Concrete and Rock*, S. P. Shah and S. E. Swartz, eds., SEM-RILEM, Houston, Tex., 138–149.

Hutchinson, J. W. (1974). "Plastic buckling." *Adv. Appl. Mech.*, 14, 67–144.

Pijaudier-Cabot, G., and Akrib, A. (1989). "Bifurcation et réponse postbifurcation de structures en béton." *Preprint, Colloquium GRECO, Rhéologie des Géomateriaux*, GRECO, Paris, France (in French).

Rots, J. G., and de Borst, R. (1987). "Analysis of mixed-mode fracture in concrete." *J. Engrg. Mech.*, ASCE, 113(11), 1739–1758.

Rots, J. G., and de Borst, R. (1989). "Analysis of concrete fracture in direct tension." *Int. J. Solids Struct.*, 25(12), 1381–1394.

Shanley, F. R. (1947). "Inelastic column theory." *J. Aero Sci.*, 14(5), 261–268.

van Mier, J. G. M. (1986). "Fracture of concrete under complex stresses." Heron, Delft, The Netherlands, 31(3), 58.

van Mier, J. G. M. (1989). "Fracture propagation in concrete under complex stress." *Fracture of Concrete and Rock; Proc., Int. Conf., SEM-RILEM*, Springer Verlag, New York, N.Y., 362–375.